



**HAL**  
open science

## Ultrasound-Induced Blood–Spinal Cord Barrier Opening in Rabbits

Anne-Sophie Montero, Franck Bielle, Lauriane Goldwirt, Adrien Lalot,  
Guillaume Bouchoux, Michael Canney, Florine Belin, Kevin Beccaria,  
Pierre-François Pradat, François Salachas, et al.

► **To cite this version:**

Anne-Sophie Montero, Franck Bielle, Lauriane Goldwirt, Adrien Lalot, Guillaume Bouchoux, et al..  
Ultrasound-Induced Blood–Spinal Cord Barrier Opening in Rabbits. *Ultrasound in Medicine & Biology*, 2019, 45, pp.2417 - 2426. 10.1016/j.ultrasmedbio.2019.05.022 . hal-03488189

**HAL Id: hal-03488189**

**<https://hal.science/hal-03488189>**

Submitted on 20 Jul 2022

**HAL** is a multi-disciplinary open access archive for the deposit and dissemination of scientific research documents, whether they are published or not. The documents may come from teaching and research institutions in France or abroad, or from public or private research centers.

L'archive ouverte pluridisciplinaire **HAL**, est destinée au dépôt et à la diffusion de documents scientifiques de niveau recherche, publiés ou non, émanant des établissements d'enseignement et de recherche français ou étrangers, des laboratoires publics ou privés.



Distributed under a Creative Commons Attribution - NonCommercial 4.0 International License



1        **ABSTRACT :**  
2  
3

4        The blood spinal cord barrier (BSCB) considerably limits the delivery and efficacy of  
5        treatments for spinal cord diseases. The blood brain barrier can be safely opened with  
6        low intensity pulsed ultrasound when microbubbles are simultaneously administered  
7        intravenously. This technique was tested on the BSCB in a rabbit model in this work.  
8        Twenty-three segments of spinal cord were sonicated with a 1MHz unfocused pulsed  
9        ultrasound device and compared to non-sonicated segments. BSCB disruption was  
10       assessed using Evan's blue dye (EBD) extravasation. Tolerance was assessed by  
11       histological analysis. An increased EBD concentration indicating BSCB disruption was  
12       clearly observed in sonicated segments compared to controls ( $p=0.004$ ). On one animal,  
13       which received 10 sonications, repetitive BSCB disruptions showed no evidence of  
14       cumulative toxicity. BSCB can be disrupted using an unfocused pulsed ultrasound  
15       device in combination with microbubbles without neurotoxicity even in case of repeated  
16       sonications.

17       **KEYWORDS:**

18       Blood spinal cord barrier, ultrasound, blood brain barrier, spinal cord, drug delivery.  
19  
20

## 1 INTRODUCTION

2  
3 Similarly to the blood–brain barrier (BBB), the blood–spinal cord barrier (BSCB) plays  
4 a protective and regulatory role for the spinal cord parenchyma. The BBB and BSCB  
5 are specialized passive and active structures between capillaries and parenchyma that  
6 protect the central nervous system from chronic exposition of potentially harmful  
7 substances. Only small (<400 Da), lipophilic compounds (2% of small molecules) can  
8 cross the BBB. The barrier function of spinal cord capillaries is based on tight junctions  
9 between nonfenestrated endothelial cells, together with the basement membrane,  
10 pericytes, and astrocytes. In addition, there are limited transport vesicles across  
11 endothelial cells of the BBB, thereby limiting transcellular transport(Abbott et al. 2010;  
12 Bartanusz et al. 2011; Pardridge 2005). For only a few substances, the BSCB has been  
13 shown to be slightly more permeable than the BBB (i.e cytokines) due to a lower cell  
14 junction protein expression (ZO-1 and occludin)(Bartanusz et al. 2011). Nevertheless,  
15 the BSCB impedes drug delivery for the treatment of various spinal cord disease  
16 including tumors, inflammatory disease (e.g. multiple sclerosis), neurodegenerative  
17 conditions (e.g. amyotrophic lateral sclerosis). Drugs, such as trophic factors have  
18 shown promising efficacy in preclinical animal models of spinal cord diseases but failed  
19 to translate in clinical trials (Kaspar et al. 2003). An important explanation is that, due  
20 to the BSCB, high doses that are not tolerated in humans would be required for the drug  
21 to effectively reach its target in the spinal cord.(Pardridge 2005)

22 Since 2001, it is known that the BBB can be safely and transiently opened using  
23 ultrasound (US) combined with intravascular systemic injection of microbubbles in pre-  
24 clinical studies(Beccaria et al. 2013; Beccaria et al. 2016; Hynynen et al. 2001). When  
25 the microbubbles pass through the ultrasound beam, they oscillate, exerting mechanical  
26 stress on the endothelium, leading to a transient increase in permeability to circulating  
27 drugs.(Burgess and Hynynen 2013; Downs et al. 2015; McDannold et al. 2005; Sheikov

1 et al. 2004) In a first-in-man safety and feasibility trial, it was shown that ultrasound  
2 induced BBB opening prior to carboplatin administration is well-tolerated in patients  
3 with recurrent glioblastoma.(Carpentier et al. 2016)

4 Our study was designed to evaluate if the BSCB could be safely disrupted using a 1 MHz  
5 unfocused pulsed ultrasound device in rabbits. BSCB disruption was quantified using  
6 Evans blue dye (EBD) extravasation. In addition, we examined if optimal acoustic  
7 parameters could be defined for sonications and evaluated the safety of multiple  
8 sonications.

## 12 MATERIAL AND METHODS

### 13 Animal protocol and surgical spinal cord exposition

14 Fifteen healthy New Zealand white rabbits, weighing 3.0–4.3 kg, were obtained from a  
15 research animal provider (CEGAV, SSC, France). Animals were housed with free  
16 access to food and water. All experimental procedures were approved by the Paris  
17 Descartes University Animal Ethics Committee (n° 2016061715547663) and were in  
18 accordance with the standards of the Guidelines for the Care and Use of Mammals in  
19 Neuroscience and Behavioral Research

20 Since ultrasound is absorbed and distorted by the spinal sagittal median posterior  
21 process, surgical removal of the bone was performed to insure reliable acoustic  
22 exposures. Animals were anesthetized by intramuscular injection of Xylazine (5 mg/kg-  
23 2% solution) and Ketamine (50 mg/kg-1000mg/10mL solution). If needed, additional  
24 injections were performed during the experiments. Animals were either ventilated with  
25 a mixture of isoflurane and oxygen using a laryngeal mask airway or allowed to  
26 spontaneously breathe ambient air. A catheter was inserted into the marginal ear vein

1 for perfusion of US-contrast agent and Evan's blue dye. The rabbit spinal cord extends  
2 from C0 to S2 (Greenaway et al. 2001). Spinal cord surgical exposition for ultrasound  
3 exposures **and controls** could be performed at multiple levels (T4, T7, T11 and L3  
4 vertebrae). On each level, the skin was infiltrated with a 1% lidocaine solution and  
5 laminectomy was performed with a Citelli punch to expose the dura-mater and allow the  
6 positioning of the ultrasound transducer. Two hours after the last sonication, animals  
7 were sacrificed by intravenous injection of pentobarbital salt (182 mg/100 mL).  
8 Laminectomies were then extended to extract the entire spinal cord for analysis of  
9 sonicated vs non-sonicated segments.

### 10 **In silico simulations of the acoustic pressure distribution**

11 From previously performed experiments in rabbit brain at our institution (Beccaria et al.  
12 2013), we tested the nominal acoustic pressure to use for safe BBB opening. In this  
13 work, we hypothesized that similar acoustic pressure levels would be safe for BSCB  
14 opening. Nevertheless, due to the close proximity of vertebral body anterior to the  
15 spinal cord, ultrasound reflection could happen, amplifying the signal intensity. To  
16 quantify this phenomenon, *in silico* treatment simulations were performed (*Figure 1*).  
17 The nominal treatment pressure amplitude delivered during treatments (*Table 1*) is  
18 defined as the pressure that would have been delivered in non-attenuative free-field  
19 conditions (water). However, the presence of distal bone in the acoustic field causes  
20 reflections and standing waves. To evaluate the actual spatial acoustic pressure  
21 distribution in the spine obtained for a given nominal pressure, simulations were  
22 conducted using a finite-difference time-domain wave propagation numerical model  
23 (Bouchoux et al. 2012). Three dimensional maps of the acoustic properties of  
24 heterogeneous media, including bone, were obtained using X-ray computed tomography  
25 scans of the C6, T4, T9, L2 vertebra of a New Zealand white rabbit. The scans were

1 segmented in three domains assigned with typical acoustic properties: soft tissues  
2 (speed of sound 1588 m/s, density 1000 kg/m<sup>3</sup>, attenuation 7 Np/m), bone (3500 m/s,  
3 2000 kg/m<sup>3</sup>, 55 Np/m), and acoustically transparent gel (1524 m/s, 1000 kg/m<sup>3</sup>, 0  
4 Np/m). (Duck 2013) The laminectomy was modeled by removing an 8 mm-diameter  
5 cylinder of bone in front of the transducer. The simulated acoustic pressure distribution  
6 during the ultrasound exposure was evaluated in a 7-mm long region of interest (ROI)  
7 inside the targeted vertebra.

### 8 **Ultrasound sonication setup**

9 The ultrasound exposure parameters used in this study (25 ms pulse duration, 1 Hz  
10 pulse repetition frequency, 1.1 MHz ultrasound frequency, 150 s treatment duration)  
11 and the ultrasound transducer geometry (1-cm diameter piezocomposite, Vermon,  
12 France) were chosen to match the device used in a clinical trial for BBB disruption by  
13 our group (Carpentier et al. 2016). The ultrasound transducer was coupled to the  
14 exposed spinal cord through a 2-cm thick 1.6-cm diameter cylinder made from an  
15 acoustically transparent gel (Aquaflex, Parker Laboratories, NJ, USA). The gelpad was  
16 used to ease the positioning of the transducer, and to place targeted tissues in the  
17 acoustic far field of the 1 MHz unfocused transducer (>15 mm) to have a more uniform  
18 acoustic field at the intended sonication site. A polyisoprene envelope (Ultracover  
19 88663, Microtek, MS, USA) covered the transducer and the gel pad to guarantee  
20 sterility. Acoustic gel was used to couple the transducer to the gel pad, the gel pad to the  
21 envelope, and the envelope to the targeted tissues.

22 The transducer was driven by a custom radiofrequency generator (CarThera, France)  
23 comprising a signal generator, a radio-frequency amplifier, an electrical power  
24 measurement system, and an electrical matching circuit. The complete setup was  
25 calibrated by placing the transducer/gel assembly in a degassed water tank at ambient

1 temperature and evaluating the relation between the electrical power and the acoustic  
2 pressure amplitude at the spatial peak measured (i.e. the nominal pressure, following  
3 our definition) with a hydrophone (HNC0200, Onda, CA, USA) mounted on a  
4 motorized positioning system (UMS, Precision Acoustics, UK). Simulated (1cm  
5 diameter piston) and measured acoustic field spatial distribution were almost identical:  
6 maximum pressure in free field, ie. nominal pressure, was measured at 15.4 mm from  
7 the transducer, vs. 15.5 mm obtained by simulation.

8 The nominal acoustic pressure varied from 0.3 MPa to 0.8 MPa according to the  
9 different experiments (*Table 1*). Right at the beginning of each sonication, a bolus of 0.2  
10 ml/kg of microbubbles (SonoVue, Bracco Imaging) was intravenously injected. As  
11 sonications were performed on each rabbit at different spinal positions, a delay of at  
12 least 15 minutes was used between each sonication to ensure washout of the contrast  
13 agent.

#### 14 **Evans Blue Dye (EBD)**

15 BSCB disruption was measured by extravasation of EBD. After the last sonication,  
16 EBD was injected intravenously at a dose of 100 mg/kg in 60 mg/mL of saline  
17 (Beccaria et al. 2013). Animals were sacrificed 120 min after the dye injection. The  
18 spinal cord was immediately extracted and the meninges were discarded.

19 Qualitative macroscopic evaluation (visual blue staining intensity) was performed on  
20 the whole spinal cord and on axial slices with respect to sonication location versus non  
21 sonicated areas. Transversal slices (3 mm long) were stored at -20°C until subsequent  
22 analysis.

23 Quantification of EBD was performed by UV-visible spectrophotometry using a Anthos  
24 *Zenyth 340 Microplate* Reader (Biochrom, Holliston, USA). The pharmacologist

1 performing the analysis (L.G) was blinded to the sonication levels. After thawing,  
2 spinal cord samples were weighed. Calibration standards and quality controls were  
3 spiked with appropriate dilutions of EBD (0 to 120 µg/mL). All samples were mixed  
4 with 100 µl of sodium chloride 0.9% (Fresenius Kabi France) and 750 µl of  
5 dimethylsulfoxide (Sigma-Aldrich, St. Louis, Missouri, United States). The mixture was  
6 then homogenized and centrifuged at 4,000 rpm for 10 min at 25°C. Absorbance in the  
7 supernatant due to EBD was measured using UV-visible spectrophotometry at a  
8 wavelength of 620 nm. Data (*table 1*) were expressed as EBD tissue concentration per  
9 wet tissue weight (µg/g). Sonicated spinal cord segments were compared to controls  
10 (non-sonicated segments).

### 11 **Histological Study**

12 Segments of the spinal cords were fixed in a 10% formalin solution for histological  
13 analysis. The neuropathologist (F.B.) was blinded to the US parameters. Axial sections  
14 of the spinal cord were embedded in paraffin. Three micron-thick sections were cut and  
15 stained by hematoxylin and eosin (H&E). Lesions were graded according to the  
16 classification proposed by Hynynen et al.(Hynynen et al. 2005) on a scale ranging from  
17 0 to 3 : “0” : no detected damage, “1” : few erythrocytes extravasation, “2” : petechial  
18 hemorrhages; mild damage to the parenchyma, and “3” : hemorrhagic or non-  
19 hemorrhagic local lesions.

### 20 **Repeated sonications and neurological evaluation**

21 Repeated (x10) sonications were performed in one rabbit on the same spinal cord  
22 segment (D4). This rabbit had only one site of laminectomy, the skin was sutured and  
23 the rabbit was woken up. A 10-day interval was kept between surgery and sonications  
24 to evaluate the toxicity of the surgery independently of ultrasound. For sonications,

1 which were all performed the same day, the rabbit was anesthetized breathing ambient  
2 air, the scar was reopened and five sonications were performed at the D4 segment with a  
3 20-minute interval between each sonication. The rabbit was woken up to allow clinical  
4 evaluation. A new anesthesia was performed, and five additional sonications were  
5 realized. Evan's blue dye was injected and the rabbit was sacrificed 120 minutes later.

6 For assessment of neurological function, a modified Tarlov scale was used (0 : no  
7 movement of the hind limbs, 1 : perceptible joint movement, 2 : good movement of the  
8 joints but inability to stand, 3 : ability to stand and walk, 4 : complete recovery = ability  
9 to hop (Tarlov 1972). Proprioception was evaluated by observing the placement of the  
10 limbs when brought to table edge. (Mancinelli 2015) Evaluation was performed before  
11 laminectomy, daily after laminectomy and 4 hours after the 5<sup>th</sup> sonication.

### 12 **Statistical analysis**

13 Statistical analysis of blue dye quantification results was performed using Graph Pad  
14 Prism 5.0 software. D'Agostino & Pearson omnibus normality test was used to  
15 determine normality of the data. To compare multiple groups, one way ANOVA with  
16 Tukey post-test was used for normal data, and Kruskal Wallis with Dunn's post test for  
17 non-parametric data. To compare two non parametric groups, Mann Whitney test was  
18 used. P-value <0.05 was considered significant. Results are presented as means ±  
19 standard error of the means (SEM).

## 20 **RESULTS**

### 21 **Simulated acoustic pressure field in the targeted tissues**

22 The simulated pressure field for an ultrasound exposure of a rabbit T4 vertebra after  
23 laminectomy through a 2-cm thick acoustically transparent gelatin pad is shown in *Figure 1*.  
24 As expected, an interference pattern typical for standing waves is clearly visible, with the

1 distance between stripes at about 0.8 mm (half of the wavelength). Reflection by the bone  
2 causes a heterogeneous pressure distribution in the targeted zone, including hotspots with  
3 acoustic pressure above the nominal pressure, which is defined as the maximum pressure  
4 amplitude measured in free-field conditions. Simulations for other vertebrae (C6, T4, T9, L2)  
5 show similar pressure field patterns. Overall,  $34\pm 6\%$  of the spinal canal ROI volume  
6 (mean $\pm$ standard deviation for the 4 evaluated vertebrae) received an acoustic pressure of 0-  
7 0.5x the nominal pressure,  $47\pm 5\%$  between 0.5-1x,  $17\pm 3\%$  between 1-1.5x, and  $2\%\pm 1\%$   
8 above 1.5x. For comparison, if ultrasound reflection and attenuation are neglected (free-field  
9 condition), 48% of the spinal-canal ROI volume would have a pressure between 0-0.5x the  
10 nominal pressure and 52% of the ROI is exposed with a pressure between 0.5-1x the nominal  
11 pressure.

12 Additional simulations were performed to evaluate a sonication through the bone, without  
13 laminectomy. The median pressure in the ROI was divided by a factor of  $3.34\pm 0.8$  because of  
14 the bone in the acoustic path. The standing wave pattern in the spinal canal was similar to the  
15 one observed with a laminectomy.

16  
17

## 18 **BSCB Opening**

19 Qualitative Macroscopic analysis showed blue colorations of the sonicated segments of the  
20 spinal cord by the EBD demonstrating the localized disruption of the BSCB (*Figure 2*). Non-  
21 sonicated spinal cord segments (controls) remained white. Similar to the effects previously  
22 observed in the brain, this coloration is more prominent in the grey matter (Beccaria et al.  
23 2013)(*Figure 2, lower*). In sagittal sections, the blue coloration of the grey matter  
24 corresponded to the length of the acoustic field but was not always observed in white matter.  
25 In some samples, the coloration was unilateral, due to the orientation of the transducer. When

1 a surgical trauma occurred, (#4, 8, 12, 30) an intense coloration was observed in both white  
2 and grey matter associated with macroscopic hemorrhage. These four segments were  
3 excluded from all the statistical efficacy analysis. In rabbits ventilated with isoflurane and  
4 oxygen a blue coloration was seen in 3/8 segments. In this group, the blue was much less  
5 intense and more limited to the grey matter than in the ambient air group. The blue coloration  
6 was observed in 11/11 sonicated segments in rabbits ventilated with ambient air including  
7 segments with low acoustic pressure (0.3MPa).

8 Quantitative spectrophotometric measurements of EBD concentration revealed a statistically  
9 significant difference in EBD concentrations between the 19 sonicated samples ( $51.4 \pm 6.1$   
10  $\mu\text{g/g}$ ) and the 7 controls ( $15.9 \pm 1.8 \mu\text{g/g}$ ),  $p=0.0004$ . (Mann Whitney test) The 11 segments of  
11 sonicated rabbits allowed to breath ambient air had a higher BSCB disruption ( $69.8 \pm 5.6$   
12  $\mu\text{g/g}$ ) compared to the 8 segments of rabbits ventilated with isoflurane/oxygen ( $26.3 \pm 2.5$   
13  $\mu\text{g/g}$ ),  $p=0.006$ . (Kruskall Wallis test – Dunn-s multiple comparaisn post test) (Figure 3).  
14 When analyzing the segments with no or minimal histological lesions (*Grade 0-1*), the EBD  
15 concentration of the 13 sonicated segments was increased when compared to the five controls  
16 ( $44.8 \pm 7.3$  vs  $15.8 \pm 2.4 \mu\text{g/g}$ ,  $p=0.004$ , Mann Whitney test). In segments with no or minimal  
17 histological lesions in rabbits breathing ambient air, EBD was even more increased ( $67.5 \pm$   
18  $8.6$ , vs  $15.8 \pm 2.4 \mu\text{g/g}$ ) compared to reabbits breathing isofluran-oxygen. None of the control  
19 segments had a BSCB disruption.

## 20 Surgical exposition and ultrasound Toxicity

21 Histological toxicity was evaluated on 23 sonicated segments and seven non sonicated  
22 segments (controls) (Table 1, figure 4). In the control segments, 2/7 (29%) had moderate or  
23 severe lesions (Grade 2-3) due to surgical trauma. In the sonicated segments, 10/23 (43%) had  
24 moderate or severe lesions (grade 2-3). Four segments (#4,8,12,30) had severe lesions (Grade

1 3), macroscopically visible, due to the surgical procedure or ultrasound toxicity. Moderate  
2 damage (*Grade 2*) was observed in 6/23 (26%) segments in the sonicated group, and in  
3 2/7(29%) segments of the control group.

#### 4 **Repeated sonication and clinical evaluation**

5 The rabbit that received 10 sonications in the same spinal segment had a clinical evaluation  
6 before and after the first five sonications. No neurological worsening was observed (Tarlov  
7 modified scale 4/4) after five sonications when compared to the neurological status after  
8 laminectomy and before ultrasound. After sonications, the rabbit was able to hop (Tarlov  
9 modified scale 4/4) and had no proprioceptive defect four hours after five sonications. After a  
10 total of 10 sonications, EBD was injected and the animal was sacrificed. There was a clear  
11 opening of the BSCB (EBD : 95µg/g) with minimal histological lesions (extravasation of less  
12 than 20 erythrocytes - Grade 1).

#### 13 **DISCUSSION**

14 This study is a proof of concept that the BSCB can be safely disrupted using a 1 MHz  
15 unfocused ultrasound device coupled with microbubbles. The optimal acoustic pressure (0.3-  
16 0.5MPa) is slightly lower to that used for BBB disruption in rabbits (0.5-0.6MPa).

17

#### 18 **Difficulties with the Rabbit Model**

19 Simulations without laminectomy showed that propagation of the 1-MHz ultrasound wave  
20 through the bone causes a reduction of acoustic pressure by a factor  $3.34 \pm 0.8$ . The very large  
21 standard deviation of this factor is due to the variability of acoustic transmission through the 4  
22 vertebrae evaluated *in silico*, and suggests a large uncertainty of the *in-situ* acoustic pressure  
23 without laminectomy. Moreover, compensating for acoustic pressure loss due to transmission  
24 through the bone would likely cause mechanical and thermal side effects in intervening

1 tissues. The simulations demonstrated that the bone thickness of the spine impedes ultrasound  
2 from reaching adequately the spinal cord, and prerequisite laminectomies were mandatory.  
3 Such laminectomies encountered several difficulties in this specific animal: highly  
4 hemorrhagic dissection of paravertebral muscles, narrowness of the spinal canal leading to  
5 possible severe spinal cord traumas during the surgical exposure (n = 4/30), and hemorrhagic  
6 lesions even on non-sonicated spinal cord segments. Larger series of animals were  
7 envisioned initially, but it appeared that the rabbit is a difficult model for spinal cord studies.  
8 In addition, due to ethical considerations for reducing the number of animals, each rabbit had  
9 multiple sites of sonication. Multiple sonication sites increased the total time of anesthesia  
10 and blood loss leading to acidosis (arterial pH often below 7 at the end of the procedure) and  
11 hyperkalemia (>7.5mmol/L). Three rabbits died of hemorrhagic shock or metabolic  
12 complication. Lastly, for the neurological evaluation, rabbits had to be kept alive after their  
13 laminectomy. Five rabbits initially received surgery for neurological evaluation but four  
14 developed a paraplegia seven to ten days after laminectomies, before any sonication due to  
15 spine instability. Only one had normal neurological status at 15 days after laminectomy and  
16 could be used for the ultrasound sonications.

17

### 18 **Impact of anesthesia**

19 Rabbits were first anesthetized with isoflurane and oxygen to limit hypoxemia. In such cases,  
20 the BSCB was poorly ( $26 \pm 2.5\mu\text{g/g}$ ) opened, and apart from surgical traumas, only one  
21 segment (#7) had a clear opening  $>30\mu\text{g/g}$ . Previous studies have shown that anesthesia  
22 agents influence the blood brain barrier disruption (McDannold et al. 2011). Isoflurane and  
23 oxygen are known to decrease the effect of the microbubbles on the blood brain barrier. This  
24 effect can be explained by vasoactive effects (including vasoconstriction, vasodilatation,  
25 blood flow) and decreases in microbubble circulation times.

1 In the second part of the experiment, we changed the ventilation method, letting rabbits  
2 spontaneously breath ambient air. With this procedure, results were much reliable. BSCB  
3 disruption was systematic (11 segments/11) and the EBD concentration was higher ( $70 \pm 5.6$   
4 vs  $26 \pm 2.5 \mu\text{g/g}$  in the isoflurane/oxygen group). The difference of Evan's blue dye  
5 concentration was highly significant between these two methods of anesthesia ( $p=0.0004$ )

6

### 7 **Evans blue dye**

8 BSCB opening was confirmed by the uptake of EBD in the sonicated segments. A blue  
9 coloration of the spinal cord was observed on the sonicated segments. There was no visible  
10 leakage of coloration on non-sonicated segments confirming the BSCB's impermeability to  
11 this dye. This macroscopic evaluation was completed and confirmed by quantitative  
12 evaluation. The EBD concentration was significantly higher in the sonicated segments  
13 compared to controls ( $51.4 \pm 6.1$  vs  $15.9 \pm 1.8 \mu\text{g/g}$   $p=0.0004$ ). Evan's blue dye is a molecule  
14 with a very high affinity for albumin, thus once injected, it binds with albumin forming a 68  
15 kDa complex which is a good model for protein permeability(Hoffmann et al. 2011; Wunder  
16 et al. 2012). In our previous results in the brain,(Beccaria et al. 2013) EBD was reliable in  
17 evaluating the BBB opening when compared to gadolinium enhancement. Indeed, just like  
18 the EBD, the gadolinium (1 kDa) uptake was limited to the sonicated location and  
19 predominate largely in the grey matter.

### 20 **Comparison to the blood brain barrier disruption**

21 An emitted acoustic pressure of between 0.3-0.4 MPa was found to be safe for disrupting the  
22 BSCB in rabbits. This pressure is slightly lower than the optimal acoustic pressure for the  
23 blood brain barrier (0.6 MPa) in a similar animal model (Beccaria et al. 2013; Beccaria et al.  
24 2016). This difference could be due to the reflection of the ultrasound wave on the opposite

1 bone, which locally increases the acoustic pressure compared to the nominal treatment  
2 pressure as shown by the simulations presented in *Figure 1*.  
3 Sonicated segments had an EBD concentration 4.4 higher than controls (69.8 vs 15.9  $\mu\text{g/g}$ ).  
4 This difference is similar to the one we previously found for the blood brain barrier: 4.1  
5 higher (26.9 vs 6.5  $\mu\text{g/g}$ ). (Beccaria et al. 2013). Other parameters such as pulse duration,  
6 pulse repetition frequency or ultrasound frequency were not changed compared to our  
7 previous studies on the brain.

8

### 9 **Tolerance of BSCB disruption by ultrasound**

10 The acoustic intensity pattern due to standing waves predicted by simulation was not observed  
11 when examining the sonicated rabbits in EBD staining. The spatial distribution of petechia  
12 and hemorrhages, when observed, was also not in a striped pattern. In fact, despite the  
13 heterogeneity of the calculated acoustic field, the EBD distribution in tissues was fairly  
14 homogeneous. This could be due to diffusion of the dye in tissues, to the heterogeneity of  
15 tissues, or to the small motions of the hand-held transducer and of the animal during  
16 ultrasound exposures, which could spread the standing-wave pattern over the treatment  
17 duration. Due to the surgical traumas mentioned above, histological safety was delicate to  
18 evaluate. Histological lesions of grade 2-3 occurred in both sonicated segments and controls,  
19 and so could be attributed primarily to surgical damages, without exclusion of potential  
20 adverse events induced by ultrasound in the sonicated segments.

21 Still, seven segments had a significant BSCB disruption with no or minimal histological  
22 lesions.

23

### 24 **Tolerance of repetitive sonications**

1 The rabbit that received five sonications in the same spinal cord segment presented no  
2 neurological adverse events. Moreover, histological analysis after 10 sonications performed  
3 the same day did not show any secondary effects. Although these data were only in one  
4 animal, it represents the first report on clinical and histological tolerance after several spinal  
5 cord sonications in an animal model. Indeed, we performed surgery on four other animals but  
6 they became paraplegic before the planned sonication due to spinal instability after  
7 laminectomy. Ethically it was difficult to add more animals. Further studies will be performed  
8 in a different animal model. Nevertheless, this data on one animal is of importance and shows  
9 the promise of this technique for treatment of spinal cord diseases. Since repetitive, monthly  
10 BBB opening has been shown to be safe in humans (Carpentier et al. 2016) it is hypothesized  
11 that this technique may also be safe for repetitive drug delivery to the spine.

## 12 **Existing literature**

13 To our knowledge, there are three reports of ultrasound-mediated BSCB disruption in the  
14 literature. These three experiments used focused ultrasound devices. The first publication  
15 involved gene delivery to the spinal cord in a rat model (Weber-Adrian et al. 2015).

16 Ultrasound was generated using a 1.114 MHz transducer for 5 minutes, with 10 ms bursts, at a  
17 repetition rate of 0.5 Hz and acoustic power of 0.73W. In this study, after one sonication, gene  
18 delivery of green fluorescent protein using a viral vector (20 nm) was increased in motor  
19 neurons (87% expression in sonicated regions vs 28% without ultrasound), and  
20 oligodendrocytes (36% vs 7%). Clinical tolerance was proven and histology at 13 days post  
21 sonication reported no toxicity.

22 The second study of BSCB disruption was also in a rat model.(Payne et al. 2017) BSCB  
23 disruption was assessed by measurement of gadolinium enhancement on magnetic resonance  
24 imaging (MRI). BSCB disruption was shown in 10/12 rats using contrast-enhanced MRI.

1 Three rats also had qualitative evaluation with Evan's Blue Dye. A correlation between  
2 Evan's Blue Dye and gadolinium was observed.

3 The third study evaluated the potential benefit of BSCB disruption on a rat model of  
4 leptomeningeal metastasis of breast cancer. (O'Reilly et al. 2018) In this study, BSCB  
5 disruption was obtain with acoustical pressure similar to those of our study (0.4MPa).

## 6 **Future developments**

7 Although surgical laminectomies are easy and routinely performed on humans without  
8 complications, further animal experiments will be performed on a different animal model such  
9 as mice, to avoid surgical laminectomy. In addition, several pathological models mimicking  
10 human diseases exist in mice for various neurological diseases such as amyotrophic lateral  
11 sclerosis.

12 In humans, the vertebral bone is thicker and more irregular than the skull which makes the trans  
13 bone passage of ultrasound very complex and hazardous. Unfocussed ultrasound could be  
14 delivered to the spinal cord with an implantable device placed directly in contact with the spinal  
15 cord.

## 16 **CONCLUSION**

17 The first safety data in a rabbit model of blood spinal cord barrier disruption using a 1 MHz  
18 unfocused ultrasound device was shown. Although the rabbit model, which required a narrow  
19 spinal canal surgical exposure induced spinal cord trauma in some animals, the BSCB  
20 opening procedure appeared to be safe in other animals, both clinically and histologically,  
21 even when repeated 10 times on the same location. Further research will be performed on  
22 mice to avoid surgical exposure and address the therapeutic potential in pathological models.

## 24 **ACKNOWLEDGMENTS**

25 Funding from the Laboratoire de Recherche en Technologies Chirurgicales Avancees, and  
26 from a donation from Miss Corinne Bouygues.

1 AS Montero received a fellowship grant from the Fondation pour la Recherche Medicale (ref  
2 DEA20170637795)

3 The authors gratefully acknowledge all members of the team of the Laboratory of Biosurgical  
4 Research, Paris, France, directed by Professor Philippe Menasche, for their help in the  
5 realization of animal experiments. The authors gratefully acknowledge Dr Lassaigne from the  
6 French National veterinary of Alfort and Dr Aurélia Klajer from the veterinary clinic  
7 Eiffelvet, Paris, France for providing rabbit CT-scans.

8

9 **DISCLOSURE**

10

11 Sorbonne University and APHP (Alexandre Carpentier is an employee) submitted a patent  
12 application on this method in 2016.

13

14

## 1 **REFERENCES**

- 2 Abbott NJ, Patabendige AAK, Dolman DEM, Yusof SR, Begley DJ. Structure and function of  
3 the blood-brain barrier. *Neurobiol Dis* 2010;37:13–25.
- 4 Bartanusz V, Jezova D, Alajajian B, Digicaylioglu M. The blood-spinal cord barrier:  
5 morphology and clinical implications. *Ann Neurol* 2011;70:194–206.
- 6 Beccaria K, Canney M, Goldwirt L, Fernandez C, Adam C, Piquet J, Autret G, Clément O,  
7 Lafon C, Chapelon J-Y, Carpentier A. Opening of the blood-brain barrier with an  
8 unfocused ultrasound device in rabbits. *J Neurosurg* 2013;119:887–898.
- 9 Beccaria K, Canney M, Goldwirt L, Fernandez C, Piquet J, Perier M-C, Lafon C, Chapelon J-  
10 Y, Carpentier A. Ultrasound-induced opening of the blood-brain barrier to enhance  
11 temozolomide and irinotecan delivery: an experimental study in rabbits. *J Neurosurg*  
12 2016;124:1602–1610.
- 13 Bouchoux G, Bader KB, Korfhagen JJ, Raymond JL, Shivashankar R, Abruzzo TA, Holland  
14 CK. Experimental validation of a finite-difference model for the prediction of  
15 transcranial ultrasound fields based on CT images. *Phys Med Biol* 2012;57:8005–  
16 8022.
- 17 Burgess A, Hynynen K. Noninvasive and Targeted Drug Delivery to the Brain Using Focused  
18 Ultrasound. *ACS Chem Neurosci* 2013;4:519–526.
- 19 Carpentier A, Canney M, Vignot A, Reina V, Beccaria K, Horodyckid C, Karachi C, Leclercq  
20 D, Lafon C, Chapelon J-Y, Capelle L, Cornu P, Sanson M, Hoang-Xuan K, Delattre J-  
21 Y, Idbaih A. Clinical trial of blood-brain barrier disruption by pulsed ultrasound. *Sci*  
22 *Transl Med* 2016;8:343re2.

1 Downs ME, Buch A, Sierra C, Karakatsani ME, Teichert T, Chen S, Konofagou EE, Ferrera  
2 VP. Long-Term Safety of Repeated Blood-Brain Barrier Opening via Focused  
3 Ultrasound with Microbubbles in Non-Human Primates Performing a Cognitive Task.  
4 PloS One 2015;10:e0125911.

5 Duck FA. Physical Properties of Tissues: A Comprehensive Reference Book. Academic  
6 Press, 2013.

7 Greenaway JB, Partlow GD, Gonsholt NL, Fisher KR. Anatomy of the lumbosacral spinal  
8 cord in rabbits. J Am Anim Hosp Assoc 2001;37:27–34.

9 Hoffmann A, Bredno J, Wendland MF, Derugin N, Hom J, Schuster T, Su H, Ohara PT,  
10 Young WL, Wintermark M. Validation of In Vivo MRI Blood-Brain Barrier  
11 Permeability Measurements by Comparison with Gold Standard Histology. Stroke J  
12 Cereb Circ 2011;42:2054–2060.

13 Hynynen K, McDannold N, Sheikov NA, Jolesz FA, Vykhodtseva N. Local and reversible  
14 blood-brain barrier disruption by noninvasive focused ultrasound at frequencies  
15 suitable for trans-skull sonications. NeuroImage 2005;24:12–20.

16 Hynynen K, McDannold N, Vykhodtseva N, Jolesz FA. Noninvasive MR imaging-guided  
17 focal opening of the blood-brain barrier in rabbits. Radiology 2001;220:640–646.

18 Kaspar BK, Lladó J, Sherkat N, Rothstein JD, Gage FH. Retrograde viral delivery of IGF-1  
19 prolongs survival in a mouse ALS model. Science 2003;301:839–842.

20 Mancinelli E. Neurologic Examination and Diagnostic Testing in Rabbits, Ferrets, and  
21 Rodents. J Exot Pet Med 2015;24:52–64.

1 McDannold N, Vykhodtseva N, Raymond S, Jolesz FA, Hynynen K. MRI-guided targeted  
2 blood-brain barrier disruption with focused ultrasound: histological findings in rabbits.  
3 *Ultrasound Med Biol* 2005;31:1527–1537.

4 McDannold N, Zhang Y, Vykhodtseva N. Blood-brain barrier disruption and vascular damage  
5 induced by ultrasound bursts combined with microbubbles can be influenced by  
6 choice of anesthesia protocol. *Ultrasound Med Biol* 2011;37:1259–1270.

7 O'Reilly MA, Chinnery T, Yee M-L, Wu S-K, Hynynen K, Kerbel RS, Czarnota GJ,  
8 Pritchard KI, Sahgal A. Preliminary Investigation of Focused Ultrasound-Facilitated  
9 Drug Delivery for the Treatment of Leptomeningeal Metastases. *Sci Rep* 2018;8:9013.

10 Pardridge WM. The Blood-Brain Barrier: Bottleneck in Brain Drug Development. *NeuroRx*  
11 2005;2:3–14.

12 Payne AH, Hawryluk GW, Anzai Y, Odéen H, Ostlie MA, Reichert EC, Stump AJ,  
13 Minoshima S, Cross DJ. Magnetic resonance imaging-guided focused ultrasound to  
14 increase localized blood-spinal cord barrier permeability. *Neural Regen Res*  
15 2017;12:2045–2049.

16 Sheikov N, McDannold N, Vykhodtseva N, Jolesz F, Hynynen K. Cellular mechanisms of the  
17 blood-brain barrier opening induced by ultrasound in presence of microbubbles.  
18 *Ultrasound Med Biol* 2004;30:979–989.

19 Tarlov IM. Acute spinal cord compression paralysis. *J Neurosurg* 1972;36:10–20.

20 Weber-Adrian D, Thévenot E, O'Reilly MA, Oakden W, Akens MK, Ellens N, Markham-  
21 Coultres K, Burgess A, Finkelstein J, Yee AJM, Whyne CM, Foust KD, Kaspar BK,

- 1 Stanisz GJ, Chopra R, Hynynen K, Aubert I. Gene delivery to the spinal cord using  
2 MRI-guided focused ultrasound. *Gene Ther* 2015;22:568–577.
- 3 Wunder A, Schoknecht K, Stanimirovic DB, Prager O, Chassidim Y. Imaging blood-brain  
4 barrier dysfunction in animal disease models. *Epilepsia* 2012;53 Suppl 6:14–21.
- 5

1 **FIGURE CAPTIONS**

2

3 **Figure 1 : Simulated acoustic field in the T4 vertebra of a 1 kg rabbit after laminectomy**

4 **Legend:** A) Typical layout used for the simulations (T4 vertebra of a 1 kg rabbit): CT scan used  
5 to determine acoustic properties and geometry of bone (grayscale axial and transverse images),  
6 tissues are replaced by acoustic coupling gel in the hatched zone to model laminectomy and in-  
7 vivo experimental conditions. B) Simulated in-situ acoustic pressure (color overlay). C) Axial  
8 profile of acoustic pressure simulated for free-field and in-situ conditions; pressures are  
9 normalized by the maximum in the free-field. D) Geometry of the simulated free-field (water)

10 **Figure 2: Macroscopic analysis of EBD distribution**

11 **Legend:** Upper panel : external view of the spinal cord. Blue coloration is observed on the  
12 three sonicated segments of the spinal cord (arrows). Lower panel : on transverse section of  
13 the sonicated segment #22 (right), the coloration predominates on the grey matter. No  
14 macroscopic blue coloration is visible on the non sonicated segment. (left)

15 **Figure 3: EBD concentration and histological status according to the different**  
16 **procedures**

17 **Legend:** Evans blue dye concentration ( $\mu\text{g/g}$ ) in the control segments (no sonication), in the  
18 sonicated segments in rabbits anesthetized with isoflurane and oxygen and in the rabbits  
19 anesthetized with ambient air. Severe histological lesions (Grade 3) have been excluded from  
20 statistical analysis and this figure because they resulted in artificially high EBD  
21 concentrations. Moderate histological lesions (Grade 2) can be found in all groups due to the  
22 model fragility and surgical exposure. Clear BSCB opening was observed without

1 *histological lesions. Performing the procedure with isoflurane and oxygen significantly*  
2 *decreased the BSCB opening. Data are presented as mean with SEM.*

3 **Figure 4: Histological aspects**

4 A-H Hemalun & eosin staining. A,C,E,G 20X magnification. Scale bar: 0,5mm. B,D,F,H 200X  
5 magnification. Scale bar 0,1mm. A,B. Absence of damage corresponded to grade 0. Erythrocytes are  
6 intravascular (arrowhead in B). C,D. Few extravasated erythrocytes are observed in grade 1  
7 (arrowhead in C). E,F. Microscopic extravasation of erythrocytes is observed in grade 2 (arrowhead in  
8 E,F). G,H. Extensive hemorrhagic lesions are observed in grade 3 (arrowheads in G,H).

9

1 **TABLE**

2 **Table 1:** experimental set up and results

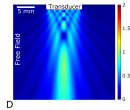
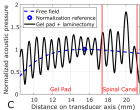
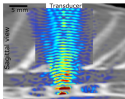
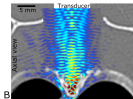
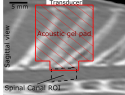
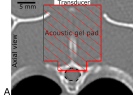
Ventilation	Sonicated Spinal cord segment Identification Nb.	Acoustic pressure (MPa)	Macroscopic Blue stain	Evan's Blue Dye (µg/g)	BSCB opening	Histology (Hynynen grade)
<i>Oxygen - Isofluran</i>	# 1	0 MPa (Control)	No	13,6	No	1
	# 2		No	17,9	No	0
	# 3		No	8,3	No	1
	# 4	0,4 MPa	Yes	76,2	Yes	3*
	# 5	0,5 MPa	No	26,5	No	0
	# 6		Yes	27,1	No	0
	# 7		Yes	39,3	Yes	0
	#8		Yes	83,3	Yes	3*
	#9		No	18,1	No	0
	#10		No	19,1	No	0
	#11		No	25,3	No	0
	#12	Yes	169,3*	Yes	3*	
	#13	0.6 MPa	No	21.9	No	1
	#14	0,8 MPa	Yes	32,7	Yes	2
<i>Ambient Air</i>	# 15	0 MPa (Control)	No	19,1	No	2
	# 16		No	16,2	No	0
	# 17		No	13,0	No	2
	# 18		No	23,0	No	1
	# 19	0,3 MPa	Yes	82,9	Yes	0
	# 20		Yes	97,7	Yes	0
	# 21		Yes	98,9	Yes	2
	# 22	0,35 MPa	Yes	61,1	Yes	0
	# 23	0,4 MPa	Yes	55,7	Yes	2
	# 24		Yes	78,5	Yes	2
	# 25		Yes	36,5	Yes	0
	# 26		Yes	60,1	Yes	0
	# 27		Yes	66,7	Yes	1
	# 28		Yes	60,9	Yes	2
	# 29		Yes	68,4	Yes	2
	# 30		0,5 MPa	Yes	163,9*	Yes
	# 31	0,4 MPa. 10 sonications	Yes	95,0	Yes	1

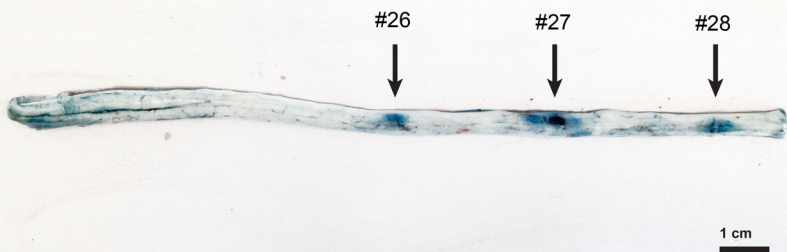
3

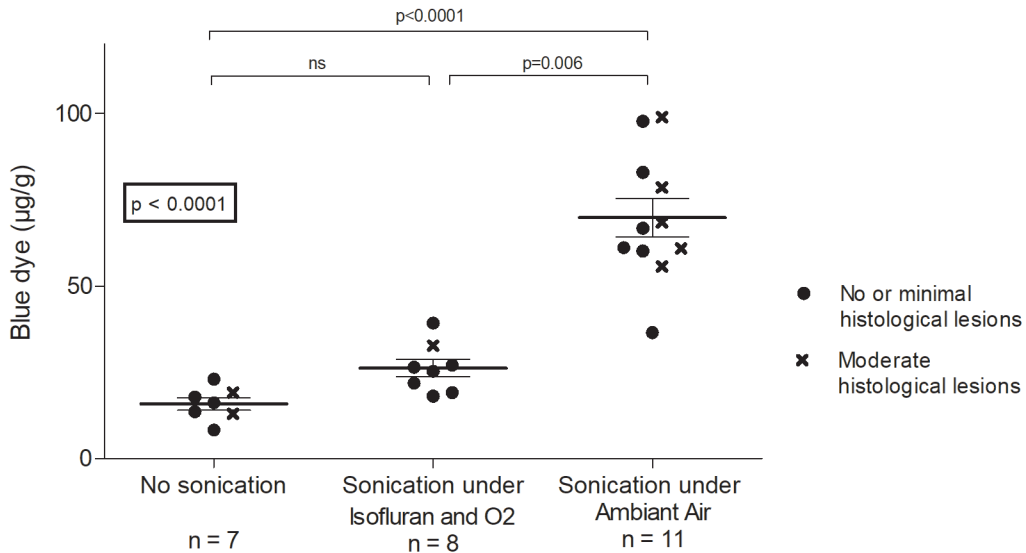
4 *In total, 23 segments had sonications and were compared to 7 controls. Sonications #4 to 14*  
5 *were performed on rabbits breathing a mixture of isofluran and oxygen while sonications*  
6 *#19 so #30 were with ambient air. 4 segments(#4#8#12#30) had severe histological lesions,*  
7 *probably due to surgical trauma. These lesions resulted in high level of EBD. These data(\*)*

1 *were excluded for statistical analysis. BSCB was determined to be opened when EBD*  
2 *concentrations exceeded 30µg/g.*

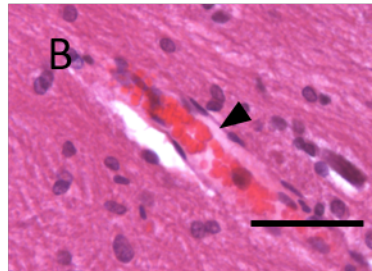
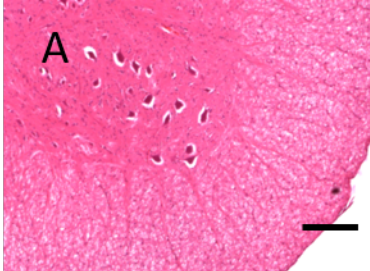
3



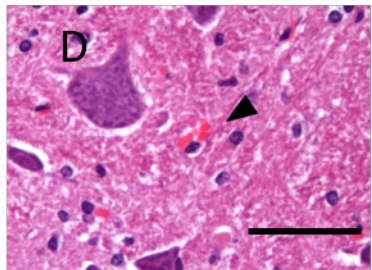
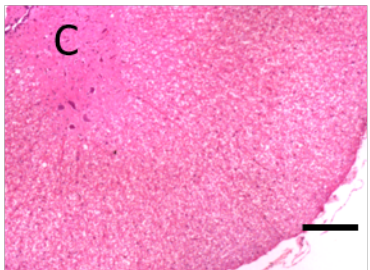




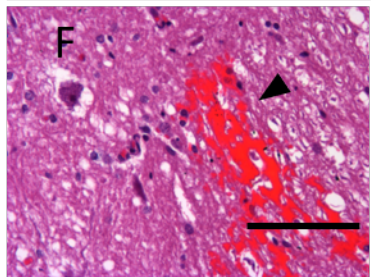
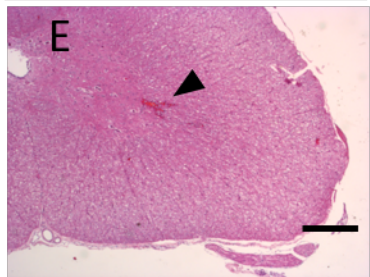
Grade 0



Grade 1



Grade 2



Grade 3

